

Cubanes

Oxygen-Atom Transfer Chemistry and Thermolytic Properties of a Di-*tert*-Butylphosphate-Ligated Mn₄O₄ CubaneKurt M. Van Allsburg,^[a, b, c] Eitan Anzenberg,^[b, c] Walter S. Drisdell,^[b, c] Junko Yano,^[b, d] and T. Don Tilley^{*[a, b, e]}*Dedicated to Manfred Scheer on the occasion of his 60th birthday*

Abstract: [Mn₄O₄{O₂P(OtBu)₂}]₆ (1), an Mn₄O₄ cubane complex combining the structural inspiration of the photosystem II oxygen-evolving complex with thermolytic precursor ligands, was synthesized and fully characterized. Core oxygen atoms within complex 1 are transferred upon reaction with an oxygen-atom acceptor (PEt₃), to give the butterfly complex [Mn₄O₂{O₂P(OtBu)₂}]₆(OPEt₃)₂. The cubane structure is restored by reaction of the latter complex with the O-

atom donor PhIO. Complex 1 was investigated as a precursor to inorganic Mn metaphosphate/pyrophosphate materials, which were studied by X-ray absorption spectroscopy to determine the fate of the Mn₄O₄ unit. Under the conditions employed, thermolyses of 1 result in reduction of the manganese to Mn^{II} species. Finally, the related butterfly complex [Mn₄O₂{O₂P(pin)}₆(bpy)₂] (pin = pinacolate) is described.

Introduction

Multinuclear transition metal complexes with bridging oxo ligands are of great interest for their ability to mediate multi-step oxidations. A particularly promising catalytic application of this redox chemistry is in artificial photosynthesis, which requires the oxidation of water by a four-electron process. Water oxidation catalysts as markedly different as the photosystem II oxygen-evolving complex (OEC),^[1] the inorganic “cobalt phosphate” electrocatalyst,^[2,3] and the ruthenium blue dimer^[4] all contain metal–oxo active sites.

The oxidation chemistry mediated by metal–oxo clusters, as in the example of water splitting, may sometimes^[5–10] (but not always)^[11,12] involve oxygen-atom transfers of the oxo ligands. Additionally, O-atom transfer processes may be required for

certain catalytic reactions, for example in olefin epoxidation^[13] and C–H hydroxylation.^[10,14–16] Therefore, metal–oxo complexes that readily donate an oxygen atom, and are regenerated by reaction with a simple oxidant (e.g., dioxygen, hydrogen peroxide, or organic peroxides) are of considerable interest.^[17]

The metal–oxo cubane cluster [Mn₄(μ₃-O)₄{O₂PPh₂}]₆ reported by Dismukes and co-workers^[18,19] is closely related to the natural OEC in structure, with alternating manganese and oxygen atoms arranged in a cube of approximate T_d symmetry. Reactivity of its core oxo ligands to generate dioxygen (on irradiation)^[20] and water (on treatment with a H-donor)^[21] comprises a partially realized water oxidation cycle. In light of previous work on the improvements made possible by immobilization of Mn–oxo clusters,^[22–24] complexes containing the Mn₄(μ₃-O)₄ cubane unit (hereafter Mn₄O₄) are promising candidates^[25,26] for molecular precursor chemistry designed to incorporate the Mn₄O₄ structure into a stable, inorganic network.

Thermolytic molecular precursors (TMPs) provide routes to inorganic materials of controlled structure.^[27–44] In one application of such precursors, a catalytic site of interest is introduced onto a support material (e.g., onto an oxide surface).^[45–49] For thermolytic molecular precursor chemistry with Mn₄O₄, an appropriate precursor should possess ligands that render the precursor complex soluble (for processing) and labile (for the low-temperature elimination of organic components). These criteria are associated with complexes of the di-*tert*-butylphosphate ligand O₂P(OtBu)₂.^[27,29,30,35,37–41]

Complexes of O₂P(OtBu)₂ with Zn,^[27] Al,^[30] Co,^[37,38,40] Cu,^[39] Cd,^[39] and Mo^[35] dissolve in organic solvents and convert upon heating to metal phosphate materials by clean elimination of isobutene and water. In addition, several di-*tert*-butylphosphate complexes of manganese have been reported. Sathiyen-

[a] K. M. Van Allsburg, Prof. T. D. Tilley
Department of Chemistry, University of California
420 Latimer Hall, Berkeley, CA 94720 (USA)
E-mail: tdtalley@berkeley.edu

[b] K. M. Van Allsburg, Dr. E. Anzenberg, Dr. W. S. Drisdell, Dr. J. Yano,
Prof. T. D. Tilley
Joint Center for Artificial Photosynthesis
Lawrence Berkeley National Laboratory (USA)

[c] K. M. Van Allsburg, Dr. E. Anzenberg, Dr. W. S. Drisdell
Materials Sciences Division
Lawrence Berkeley National Laboratory (USA)

[d] Dr. J. Yano
Physical Biosciences Division
Lawrence Berkeley National Laboratory (USA)

[e] Prof. T. D. Tilley
Chemical Sciences Division
Lawrence Berkeley National Laboratory (USA)

Supporting information for this article is available on the WWW under
<http://dx.doi.org/10.1002/chem.201406114>.

diran and Murugavel described $[\text{Mn}\{\text{O}_2\text{P}(\text{OtBu})_2\}_2]_n$, a coordination polymer, and $[\text{Mn}_4(\mu_4\text{-O})\{\text{O}_2\text{P}(\text{OtBu})_2\}_6]$, an oxo-bridged manganese tetramer.^[39] These complexes undergo thermal elimination of isobutene below 200 °C, and further heating to 450 °C produces $\text{Mn}(\text{PO}_3)_2$, $\text{Mn}(\text{PO}_3)_3$, and $\text{Mn}_2\text{P}_2\text{O}_7$.

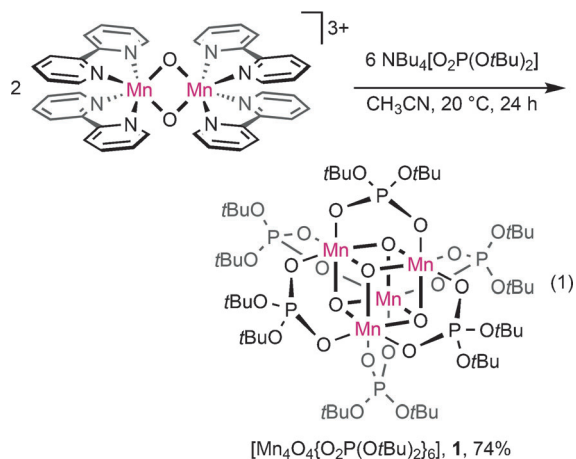
A related ligand of potential utility in precursor chemistry, the cyclic pinacol phosphate $\text{O}_2\text{P}(\text{pin})$, has yet to be explored in thermolytic routes to phosphate materials. This ligand might be expected to provide low-temperature eliminations of 2,3-dimethylbutadiene to yield the phosphate material after appropriate processing. To our knowledge, this ligand has not previously been employed in transition metal chemistry.

Herein, the synthesis, properties, and reactivity of a new molecular precursor cubane, $[\text{Mn}_4\text{O}_4\{\text{O}_2\text{P}(\text{OtBu})_2\}_6]$ (**1**) are described. Attempted isolation of a cubane complex containing the $\text{O}_2\text{P}(\text{pin})$ ligand instead gave a “butterfly” complex, $[\text{Mn}_4\text{O}_2\{\text{O}_2\text{P}(\text{pin})\}_6(\text{bpy})_2]$ (**2**). An O-atom transfer from complex **1** to triethylphosphine produced a second butterfly structure, $[\text{Mn}_4\text{O}_2\{\text{O}_2\text{P}(\text{OtBu})_2\}_6(\text{OPEt}_3)_2]$ (**3**). Interestingly, the cubane structure **1** is regenerated by the addition of PhIO (an O-atom donor) to complex **3**. Finally, thermolyses of complex **1** under several conditions were found to invariably give inorganic phosphate materials with substantial reduction to Mn^{II} .

Results and Discussion

Synthesis and properties of the Mn_4O_4 cubane complex **1**

The manganese–oxo complex $[\text{Mn}_4\text{O}_4\{\text{O}_2\text{P}(\text{OtBu})_2\}_6]$ (**1**) was prepared using a procedure analogous to that reported for $[\text{Mn}_4\text{O}_4\{\text{O}_2\text{PPh}_2\}_6]$.^[18] Two equivalents of the mixed-valence dimanganese complex $[(\text{bpy})_2\text{Mn}(\mu_2\text{-O})_2\text{Mn}(\text{bpy})_2](\text{ClO}_4)_3$ ^[50] reacted in acetonitrile with $\text{NBu}_4[\text{O}_2\text{P}(\text{OtBu})_2]$ ^[51] [Eq (1)]. Since the ¹H NMR signals for ligands of both the Mn_2O_2 precursor and the Mn_4O_4 product are paramagnetically broadened, reaction progress was monitored by integration of the signals for diamagnetic species in solution. When the expected quantity of 2,2'-bipyridine (bpy) was observed (as indicated by the bpy/ NBu_4 ratio), the reaction was considered complete (about 24 h). Evaporation of solvent produced a red solid, which readily dissolved in organic solvents but was difficult to separate from bpy. The bpy was carefully removed from the product by



sublimation under high vacuum at 70 °C. Analytically pure red crystals of complex **1** were then grown in 74% yield by cooling a concentrated hexane solution to –30 °C.

The ¹H NMR spectrum of compound **1** in $[\text{D}_2]$ dichloromethane contains a single, broad peak with a half-height width of 190 Hz at 20 °C. No ¹³C or ³¹P NMR signals were detected over the temperature range of 238–303 K. High-resolution, positive-mode electrospray ionization time-of-flight mass spectrometry (ESI-TOF-MS) reveals a weak peak corresponding to oxidized complex **1**⁺ ($m/z = 1538.31$).

The structure of complex **1**, as determined by single-crystal X-ray diffraction at 100 K, is shown in Figure 1. Two independ-

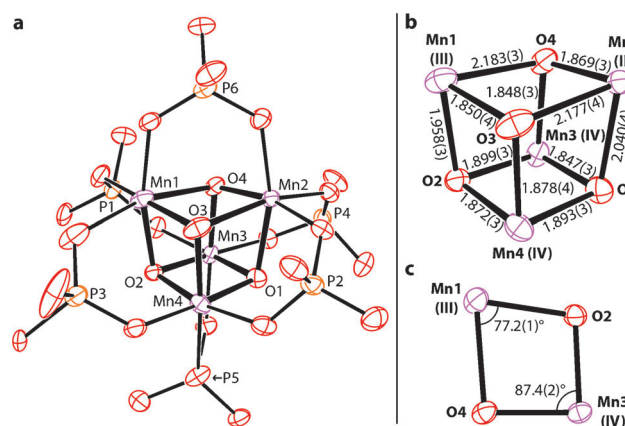


Figure 1. a) The structure of $[\text{Mn}_4\text{O}_4\{\text{O}_2\text{P}(\text{OtBu})_2\}_6]$ (**1**). For the first of the two molecules in the asymmetric unit, thermal ellipsoids are set at 50% probability. Carbon and hydrogen atoms are omitted for clarity; b) Detailed structure of the Mn_4O_4 core, including M– O_{oxo} distances in Å; c) The Mn_2O_2 face containing Mn1 and Mn3, including angles in degrees.

ent molecules in the asymmetric unit possess similar structures, containing an Mn_4O_4 core with each Mn_2O_2 face of the cube bridged by a $\text{O}_2\text{P}(\text{OtBu})_2$ ligand (Figure 1 a). Both molecules exhibit Mn– O_{oxo} bond length alternations that reflect the presence of two Mn^{III} and two Mn^{IV} centers. Relatively short and uniform Mn– O_{oxo} bond lengths are associated with the Mn^{IV} centers (av. 1.88 ± 0.04 Å; Figure 1 b), whereas the Mn^{III} sites exhibit a wide range of distances (1.850(4)–2.236(3) Å) that are longer on average (av. 2.01 ± 0.15 Å) and consistent with an expected Jahn–Teller distortion for d^4 . Furthermore, the $\text{O}_{\text{oxo}}\text{-Mn-O}_{\text{oxo}}$ angles for the Mn^{III} sites (av. $80 \pm 2^\circ$) deviate more dramatically from an idealized cubic geometry than do the angles for the Mn^{IV} sites (av. $85 \pm 2^\circ$). This trend is illustrated by the depiction of a particular Mn_2O_2 face in Figure 1 c.

The clear distinction of Mn^{III} and Mn^{IV} sites in the structure of cluster **1** contrasts with what has been reported previously for the structure $[\text{Mn}_4\text{O}_4\{\text{O}_2\text{PPh}_2\}_6]$, which appears to possess equivalent Mn centers.^[18] This difference might be attributed to the temperatures for data collection (100 K for **1**; 298 K for $[\text{Mn}_4\text{O}_4\{\text{O}_2\text{PPh}_2\}_6]$); however, a later determination of the structure of $[\text{Mn}_4\text{O}_4\{\text{O}_2\text{PPh}_2\}_6]$ at 150 K also revealed roughly equivalent Mn–O bond lengths in the cube.^[52] Interestingly, the structure determined for $[\text{Mn}_4\text{O}_4\{\text{O}_2\text{P}(p\text{-OMeC}_6\text{H}_4)_2\}_6]$ at 120 K contains Mn^{III} and Mn^{IV} sites that are well resolved.^[53]

Compound **1** undergoes electrochemical oxidation and reduction events in organic solution at approximately the same potentials as does $[\text{Mn}_4\text{O}_4(\text{O}_2\text{PPh}_2)_6]$, but, in contrast to the phosphinate complex, no reversible waves suggesting a stable ion (1^+ or 1^-) were observed.

Like $[\text{Mn}_4\text{O}_4(\text{O}_2\text{PPh}_2)_6]$,^[18] complex **1** is EPR-silent in toluene solution and in the solid state from 10 to 300 K. Variable-temperature SQUID magnetic susceptibility data (SQUID=superconducting quantum interference device) collected on complex **1** reveals a μ_{eff} of 7.3 Bohr magnetons (BM) at 300 K, which is significantly lower than the value predicted by the spin-only formula (15.0 BM) but consistent with the value reported for $[\text{Mn}_4\text{O}_4(\text{O}_2\text{PPh}_2)_6]$ (7.6 BM).^[52] This observation indicates extensive magnetic coupling within the cubane.

In contrast to $[\text{Mn}_4\text{O}_4(\text{O}_2\text{PPh}_2)_6]$, $[\text{Mn}_4\text{O}_4(\text{O}_2\text{P}(\text{OtBu})_2)_6]$ (**1**) is highly soluble in a variety of organic solvents, including pentane, toluene, diethyl ether, THF, acetonitrile, and dichloromethane. This property makes complex **1** amenable to applications involving solution processing. However, exposure of complex **1** to air resulted in slow decomposition through an apparent reaction with atmospheric moisture. It was, therefore, handled and stored under dry conditions. The moisture sensitivity of complex **1** differs from the properties of the $\text{Mn}^{\text{II}}\text{-O}_2\text{P}(\text{OtBu})_2$ polymer $[\text{Mn}(\text{O}_2\text{P}(\text{OtBu})_2)_2]_n$.^[39]

Synthesis and properties of the Mn_4O_2 butterfly complex **2**

Treatment of $[\text{Mn}_2\text{O}_2(\text{bpy})_4](\text{ClO}_4)_3$ with six equivalents of the tetrabutylammonium salt of pinacol phosphate ($\text{NBu}_4[\text{O}_2\text{P}(\text{pin})]$), under conditions identical to those used to prepare complex **1**, did not produce an Mn_4O_4 cubane. Instead, a red solid that precipitated from the brown acetonitrile reaction mixture was subsequently characterized as the butterfly compound $[\text{Mn}_4\text{O}_2(\text{O}_2\text{P}(\text{pin}))_6(\text{bpy})_2]$ (**2**; by X-ray crystallography; see below). This complex was obtained in 40% yield; however, the synthetic procedure was found to be sensitive to an impurity in the $\text{NBu}_4[\text{O}_2\text{P}(\text{pin})]$ reagent. Since rigorously purified $\text{NBu}_4[\text{O}_2\text{P}(\text{pin})]$ failed to give complex **2** (no solid precipitated from the acetonitrile reaction mixture, and removal of solvent followed by extraction with hexane, toluene, diethyl ether, and dichloromethane did not provide **2**), it seemed that the original batch of $\text{NBu}_4[\text{O}_2\text{P}(\text{pin})]$ may have contained an O-atom-acceptor species as an impurity. Support for this hypothesis was obtained by addition of two equivalents of PPh_3 (as an O-atom acceptor)^[10] to the reaction mixture. In this optimized synthesis [Eq. (2)], complex **2** was obtained as a red solid in 67% yield. In an attempt to convert **2** to a more oxidized cluster, for example, a cubane analogous to **1**, addition of iodobenzene to **2** (20°C , CD_2Cl_2) led to no reaction over 12 days.

The ^1H NMR spectrum of compound **2** in $[\text{D}_2]$ dichloromethane contains a single, broad peak with a half-height width of 360 Hz at 20°C . No ^{13}C or ^{31}P NMR signals were detected at any temperature. ESI-TOF-MS reveals a weak peak corresponding to oxidized complex $\mathbf{2}^+$ ($m/z=1639.17$).

The structure of complex **2**, as revealed by X-ray crystallography at 100 K, contains an Mn_2O_2 diamond core flanked by

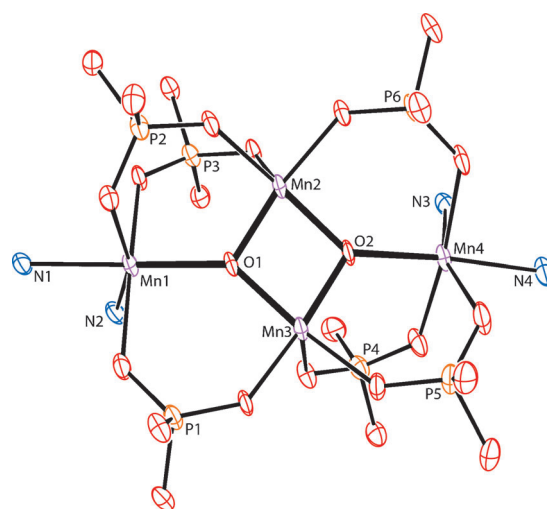
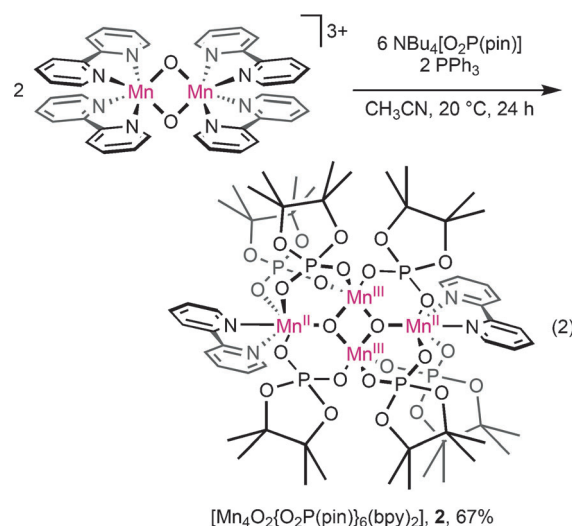


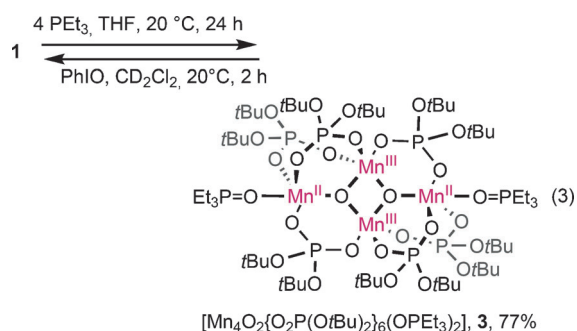
Figure 2. The structure of $[\text{Mn}_4\text{O}_2(\text{O}_2\text{P}(\text{pin}))_6(\text{bpy})_2]$ (**2**). Thermal ellipsoids are set at 50% probability. Carbon and hydrogen atoms are omitted for clarity.

two outer Mn centers (Figure 2). Both inner Mn centers are coordinated by two oxo and three $\text{-OPO}(\text{pin})$ oxygen donors and exhibit a distorted square pyramidal geometry, with $\text{O}_{\text{apical}}\text{-Mn-O}_{\text{basal}}$ angles ranging from $90.1(1)^\circ$ to $111.4(1)^\circ$. The outer Mn centers, each ligated by one oxo ligand, three phosphate oxygen atoms, and one bipyridine, are in a pseudo-octahedral coordination environment. Comparison of Mn–O bond lengths in the structure allows assignment of discrete Mn^{II} and Mn^{III} centers. Shorter Mn– O_{oxo} (av. $1.80 \pm 0.05 \text{ \AA}$) and Mn– $\text{O}_{\text{phosphate}}$ (av. $1.98 \pm 0.11 \text{ \AA}$) distances observed for the inner Mn sites are consistent with Mn^{III} , whereas longer Mn– O_{oxo} (av. $2.01 \pm 0.03 \text{ \AA}$) and Mn– $\text{O}_{\text{phosphate}}$ (av. 2.15 ± 0.02) distances for the outer sites indicate Mn^{II} .

A previously reported complex, $[\text{Mn}_4\text{O}_2(\text{O}_2\text{CCH}_3)_6(\text{bpy})_2]$, is a structural analogue of complex **2** with similar connectivity and the same arrangement of Mn^{II} and Mn^{III} sites.^[54] The complexes differ in that the carboxylate cluster has an imposed center of inversion, whereas the phosphate cluster **2** has approximate twofold rotational symmetry.

O-atom transfer from cubane **1** to triethylphosphine

It was of interest to investigate cubane **1** as a possible source of O atoms in oxidation chemistry. Thus, an attempt was made to observe O-atom transfer from **1** to triethylphosphine with formation of OPET_3 . Complex **1** reacted upon addition of four equivalents of triethylphosphine to generate the butterfly complex $[\text{Mn}_4\text{O}_2\{\text{O}_2\text{P}(\text{OtBu})_2\}_6(\text{OPET}_3)_2]$ (**3**; Eq. (3)). After removal of solvent and unreacted phosphine, red-violet crystals of complex **3** grew from hexane solution in 77% yield. As in the parent cubane **1**, only broadened signals were detected by ^1H NMR spectroscopy and no ^{13}C or ^{31}P NMR signals were detected. A broad, unresolved ^1H NMR peak detected in $[\text{D}_2]$ dichloromethane at 20°C had a half-height width of 640 Hz. As determined by X-ray crystallography (see below), two oxo ligands were removed from **1** to form the butterfly complex **3**, shown in Eq. (3). Note that this process differs from that reported by Agapie and co-workers, in which an Mn_4O_4 cubane reacted with trimethylphosphine via transfer of one oxygen atom, to produce an Mn_4O_3 partial cubane and OPMe_3 .^[55] Also, complex **1** did not react with PPh_3 in THF at 80°C over 6 h, nor with Et_2S in THF at room temperature over 20 h.



Product **3** crystallized in space group $P\bar{1}$ with inversion symmetry imposed on the cluster and $Z=1$ (Figure 3). The ar-

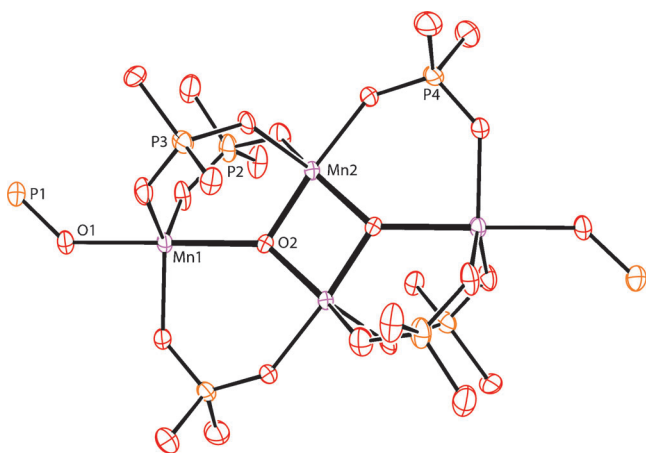


Figure 3. The structure of $[\text{Mn}_4\text{O}_2\{\text{O}_2\text{P}(\text{OtBu})_2\}_6(\text{OPET}_3)_2]$ (**3**). Thermal ellipsoids are set at 50% probability. Carbon and hydrogen atoms are omitted for clarity.

angement of an inner $\text{Mn}^{\text{III}}_2\text{O}_2$ diamond, two outer Mn^{II} sites, and six bridging phosphate ligands observed for complex **2** is preserved in complex **3**. The complexes differ in the replacement of bpy with OPET_3 as the terminal ligand, which results in all four metal centers of complex **3** being five-coordinate. Using the τ bond-angle parameter proposed by Addison et al.,^[56] the inner Mn sites of complex **3** were found to have a geometry intermediate between square pyramidal and trigonal bipyramidal ($\tau=0.55$). These inner centers are associated with Mn^{III} on the basis of their shorter $\text{Mn}-\text{O}_{\text{oxo}}$ (1.840(3), 1.860(2) Å) and $\text{Mn}-\text{O}_{\text{phosphate}}$ (av. 2.03 ± 0.06 Å) distances. The outer Mn sites possess a trigonal bipyramidal geometry and longer $\text{Mn}-\text{O}_{\text{oxo}}$ (2.179(2) Å) and $\text{Mn}-\text{O}_{\text{phosphate}}$ (av. 2.06 ± 0.01 Å) distances, indicating Mn^{II} . A previously described complex, $[\text{Mn}_4\text{O}_2\{\text{O}_2\text{CCPh}_3\}_6(\text{OEt}_2)_2]$, is a structural analogue of **3**.^[57]

Interestingly, the complete Mn_4O_4 cubane structure of complex **1** was restored by the stoichiometric reaction of complex **3** with iodobenzene, an O-atom donor. In $[\text{D}_2]$ dichloromethane solution, the reaction was monitored by ^1H NMR spectroscopy, using ferrocene as an internal standard. This reaction occurred over about 2 h, as indicated by the integration values for signals of **3**, **1**, and PhI (a byproduct), with a single apparent Mn product (**1**) and a final conversion of 55–65%. The identity of the product **1** was confirmed by ESI-TOF-MS. Note that the interconversion of **1** and **3** is related to the “double-pivot” mechanism previously proposed for water oxidation in the photosystem II OEC,^[58,59] although this mechanism is inconsistent with current structural models.^[60–62]

Thermolysis of complex **1** to manganese phosphate materials

The potential use of $[\text{Mn}_4\text{O}_4\{\text{O}_2\text{P}(\text{OtBu})_2\}_6]$ (**1**) as a thermolytic precursor to manganese phosphate materials was examined. Thermogravimetric analysis (TGA) of complex **1** revealed a slow thermolytic process at 100°C . Heating at a constant rate of $5^\circ\text{C}\text{min}^{-1}$ under flowing N_2 resulted in a sharp mass loss of 44% from $130\text{--}150^\circ\text{C}$ (Figure 4), consistent with elimination of isobutene. A gradual process, assigned as elimination of water through cross-linking of phosphate groups, continued from this temperature up to approximately 500°C . The volatile thermolysis products at 200°C were confirmed to be isobutene

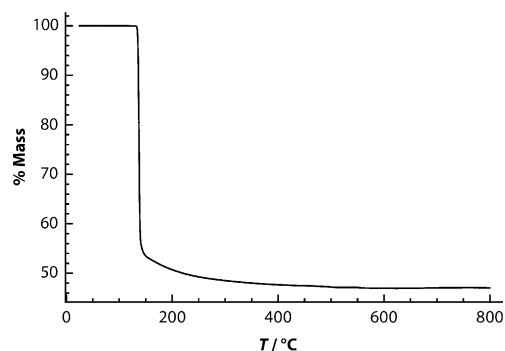


Figure 4. Thermogravimetric analysis (TGA) trace of complex **1** on heating at $5^\circ\text{C}\text{min}^{-1}$ to 800°C under flowing N_2 .

(10.3 equivalents) and water (1.0 equivalents) by vacuum transfer into a cooled NMR tube containing $[D_8]$ toluene and ferrocene as an internal standard.

Bulk crystallization appears to occur between 550 °C and 800 °C, as samples heated to the former temperature during TGA do not exhibit any peaks in their powder XRD spectra. Samples heated to 800 °C, by contrast, display XRD peaks consistent with a manganese metaphosphate/pyrophosphate mixture (Figure 5), $2Mn(PO_3)_2$ – $Mn_2P_2O_7$ ($Mn_4P_6O_{19}$).^[63,64] This ratio of phosphates is in agreement with the stoichiometry of Mn and P in complex **1** and with the final ceramic yield at 800 °C (expected: 46.1%; observed: 47.0%).

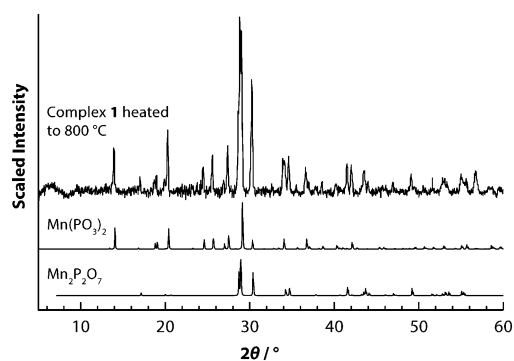


Figure 5. Powder XRD patterns: Compound **1** heated to 800 °C during TGA (top, background removed by fitting), manganese metaphosphate (middle, PDF Card 04-010-8577),^[63] and manganese pyrophosphate (bottom, PDF Card 00-035-1497).^[64]

The solution-phase transformation of cubane **1** to an inorganic substance was investigated by heating a red solution of the complex in toluene at 160 °C for 30 min. A brown gel formed, from which solvent was removed by decantation and application of vacuum. The resulting brown solid gave rise to no peaks by powder XRD after preparation, and no XRD peaks were detected after heating the gel for 5 h at 500 °C under flowing O_2 . A sample calcined for 5 h at 800 °C under O_2 displayed an XRD pattern similar to that in Figure 5, indicating a mixture of Mn metaphosphate and pyrophosphate.^[63,64]

Solution-phase co-thermolyses of compound **1** with other oxide precursors were investigated, as a potential means for isolation of $\{Mn_4O_4(PO_4)_6\}$ units within an oxide matrix. For this purpose, the thermolytic precursors $[Al(OiPr)_2O_2P(OtBu)_2]_4$ (to aluminophosphate)^[30] and $Zr[OSi(OtBu)_3]_4$ (to zirconia-silica)^[28,65] were used, given their low-temperature clean transformations to inorganic materials. In a typical preparation, compound **1** and the added precursor (in a 1:10 mass ratio) were heated in toluene to 160 °C for 30 min. The resultant gels crystallized on heating to 800 °C under flowing O_2 , but no evidence of any mixed-metal phase was observed. The powder XRD patterns reflect the presence of a combination of the expected materials from single-component thermolyses. This finding indicates that distinct crystalline phases of Mn metaphosphate and pyrophosphate, as well as the accompanying $AlPO_4$ or $ZrO_2 \cdot 4SiO_2$, had formed.^[28,30]

The thermolytic properties of complex **2**, as investigated by TGA, indicate that a clean low-temperature transformation (to preserve the key structural unit of the precursor)^[36] to a purely inorganic phosphate material does not occur (for details, see the Supporting Information), presumably due to the presence of the bipyridine ligands.

X-ray absorption spectroscopy of materials derived from precursor **1**

The fate of the Mn_4O_4 cubane unit in the aforementioned phosphate materials is of interest in the context of general strategies for metal-oxo cluster immobilization. Useful protocols will deliver the core structure of interest, intact, into a robust supporting material. It is therefore critical to develop reliable methods for identification of intact cubanes in molecular and extended materials.

Since both $[Mn_4O_4\{O_2P(OtBu)_2\}_6]$ (**1**) and $[Mn_4O_4\{O_2PPh_2\}_6]$ contain the Mn_4O_4 unit to be identified in new inorganic materials, any spectroscopic feature appearing in both might serve as a characteristic signature for the Mn_4O_4 cube. Routine magnetic (NMR, EPR), vibrational (infrared, Raman, confocal resonance Raman), and electronic (UV/Vis, X-ray photoelectron) spectroscopies revealed no clear identifying feature shared by the two complexes, so Mn X-ray absorption spectroscopy (XAS) was employed.

Mn XAS on $[Mn_4O_4\{O_2P(OtBu)_2\}_6]$ (**1**) and $[Mn_4O_4\{O_2PPh_2\}_6]$ reveals several identifying features that collectively signify the presence of an Mn_4O_4 cube. First, the Mn K-edge energy, associated with formal Mn oxidation state, is consistent between the two cubane complexes (Figure 6a). Taken as the zero crossing of the second derivative X-ray absorption near-edge structure (XANES) spectrum, the edge energies of 6550.15 eV for complex **1** and 6550.58 eV for $[Mn_4O_4\{O_2PPh_2\}_6]$ fall in the same energy range as that reported previously for a manganese(3.5) cubane.^[66] Second, information on Mn coordination environment from extended X-ray absorption fine-structure (EXAFS) spectroscopy (Figure 6b) is consistent between the two complexes. Furthermore, a crystal structure-based fit to the Fourier transform EXAFS spectrum of **1** produces good agreement (Figure 6c). Finally, for comparison, the XAS signature of the butterfly complex **3** is included in Figure 6a,b. Its edge energy (6546.89 eV) and FT-EXAFS spectrum differ markedly from those of $[Mn_4O_4\{O_2P(OtBu)_2\}_6]$ (**1**) and $[Mn_4O_4\{O_2PPh_2\}_6]$.

The application of XAS to the materials produced by thermolyses indicates that in all cases the Mn_4O_4 cubane unit is transformed. This result is exemplified by data collected for two thermolysis products that provided good EXAFS signals; the dried gel produced from solution-phase thermolysis of complex **1** and the dried gel obtained from co-thermolysis of 1:10 complex **1** and $Zr[OSi(OtBu)_3]_4$. For both materials, a sharp XANES peak and edge energy shift (to 6546.70–6546.93 eV) reveal reduction of Mn centers from the precursor oxidation state of $Mn^{3.5}$ to Mn^{II} (Figure 7a). Furthermore, a sharp FT-EXAFS peak associated with Mn–Mn and Mn–P scattering in complex **1**, between 2 and 3 Å in apparent distance, is not evi-

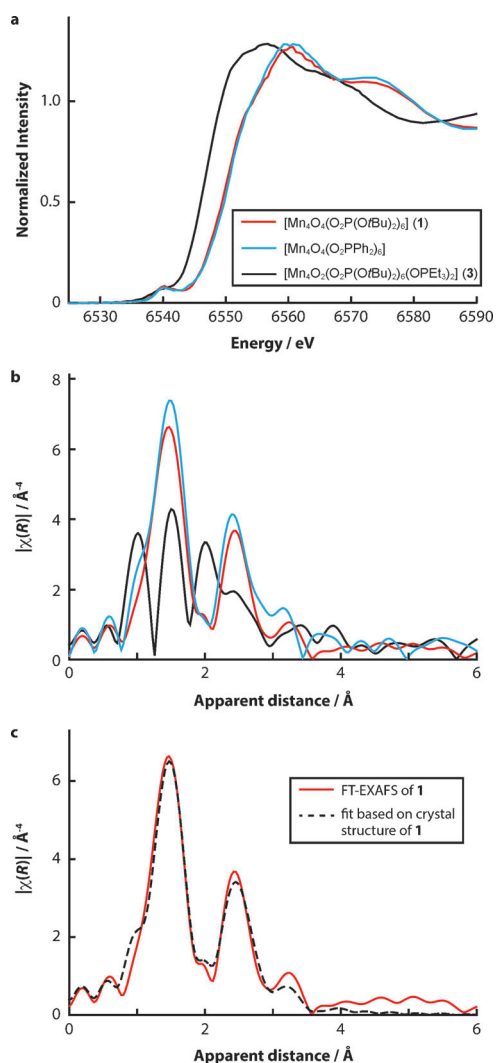


Figure 6. Mn K-edge absorption spectra of complex 1 (red), $[\text{Mn}_4\text{O}_4(\text{O}_2\text{PPh}_2)_6]$ (blue), and complex 3 as an Mn_4 non-cubane reference compound (black): a) XANES; b) FT-EXAFS; c) FT-EXAFS curve-fit results for complex 1 only.

dent in the two thermolytic products (Figure 7b). The loss of this peak is consistent with breakup of the Mn_4O_4 units into Mn sites with varying coordination environments and (on average) long Mn–Mn distances. Taken together, these results suggest decomposition of the Mn_4O_4 cluster in 1 to isolated Mn^{II} sites.

In light of XAS evidence for thermolytic reduction of the Mn^{IV} sites in $[\text{Mn}_4\text{O}_4(\text{O}_2\text{P}(\text{O}t\text{Bu})_2)_6]$ (1) to isolated Mn^{II} , the possible evolution of dioxygen from the complex's core oxo ligands was considered.^[20,67] To investigate this possibility, mass spectral analysis of volatile thermolysis products was employed. Under an atmosphere of argon (150 Torr), a sample of complex 1 was heated to $170 \pm 10^\circ\text{C}$ for one hour. The flask was then connected to a vacuum system designed for controlled delivery of headspace gas to a quadrupole mass spectrometer. Although up to two equivalents of dioxygen might be expected from the four oxo ligands in complex 1, only 0.36(2) equivalents were detected.

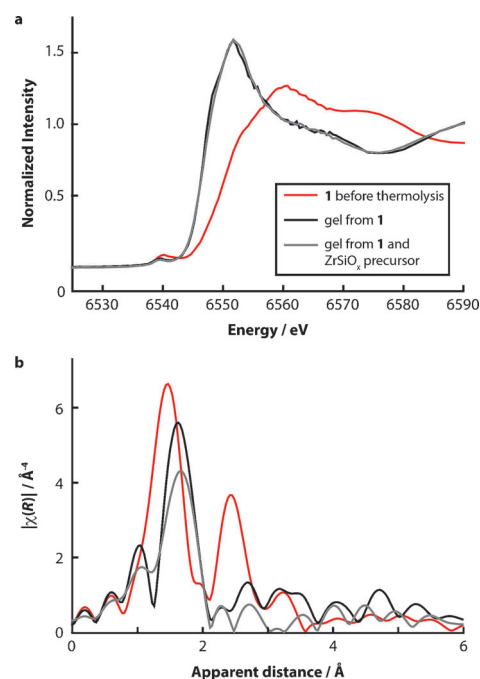


Figure 7. Mn K-edge absorption spectra of complex 1 (red), a gel produced by solution-phase thermolysis of 1 (black), and a gel produced by solution-phase co-thermolysis of a 1:10 ratio of complex 1 and $\text{Zr}[\text{OSi}(\text{O}t\text{Bu})_3]_4$ (grey): a) XANES; b) FT-EXAFS.

Electrochemical water oxidation activity of complex 1 and thermolytic materials

The ultimate aim of this work is the preparation of efficient water oxidation catalysts from Mn_4O_4 cubane molecular precursors. Unfortunately, none of the precursors or inorganic materials described herein are significant catalysts for water oxidation under the conditions employed. Electrode–adsorbate assemblies were prepared by spin-coating, drop-casting, immersion in a precursor solution during thermolysis, attempted ligand exchange (electrostatic anchoring) with surface OH groups, and organic linker (PO_3 -terminated) strategies. Cyclic voltammetry and electrolysis were performed in 1 M KOH solution. In all cases, overpotentials (relative to the thermodynamic potential for water oxidation) exceeded one volt for electrochemical water oxidation at a current density of 10 mA cm^{-2} .

Conclusions

The solubility properties of complex 1 are quite conducive to physical characterization and reactivity studies. Most significantly, this work demonstrates a structural change of the Mn_4O_4 cubane core upon transfer of two oxygen atoms to triethylphosphine. Reactivity of the resulting butterfly complex 3 with an oxygen-atom donor to regenerate the original cubane structure supports the possibility of oxidation catalysis by complexes of this type. The properties of 1 also indicate that it has potential as a precursor to materials containing the inorganic $\{\text{Mn}_4\text{O}_4(\text{PO}_4)_6\}$ unit. However, under the few conditions examined so far, the thermolytic process that converts 1 to an inorganic material is accompanied by reduction of the manganese

centers and a structural change that degrades the cubane unit. Future efforts will focus on precursor transformations (and related molecular precursors) that preserve the oxidation state and structure of the inorganic Mn_4O_4 core while delivering it to a surface or thin film. In this regard, the identification of XANES and EXAFS features for molecular manganese cubanes should greatly enable the pursuit of inorganic materials containing discrete M_4O_4 cubane units.

Experimental Section

General procedures: Unless otherwise noted, compounds were synthesized and manipulated under air-free conditions, using either a Vacuum Atmospheres drybox or standard Schlenk techniques under a dry nitrogen atmosphere. Dry solvents were obtained using a commercial solvent purification system from JC Meyer Solvent Systems.

NMR spectra were recorded on a Bruker Avance III 500 MHz spectrometer. All spectra were referenced to residual internal solvent signals. TGA was performed using a Thermal Analysis Q50 TGA unit. Powder XRD data were collected using a Rigaku SmartLab diffractometer.

The mixed-valence dimanganese complex $[(bpy)_2Mn(\mu_2-O)_2Mn(bpy)_2](ClO_4)_3$ ^[50] and the phosphate ligands $NBu_4[O_2P(OtBu)_2]$ ^[51] and $NBu_4[O_2P(pin)]$ ^[68] were synthesized as described previously.

$[Mn_4O_4\{O_2P(OtBu)_2\}_6]$ (1): A procedure similar to that described in reference [18] was used. The dimanganese complex $[(bpy)_2Mn(\mu_2-O)_2Mn(bpy)_2](ClO_4)_3$ (1.32 g, 1.24 mmol), $NBu_4[O_2P(OtBu)_2]$ (1.68 g, 3.72 mmol), and acetonitrile (75 mL) were stirred at 20 °C for 24 h. During this time, the mixture's appearance changed from a green-brown suspension to a deep red solution, and the ¹H NMR ratio of free 2,2'-bipyridine *Ar-H* to tetrabutylammonium $-CH_2-$ reached 1:3, indicating reaction completion. Removal of acetonitrile under reduced pressure, extraction with hexane (40 mL), filtration, and removal of hexane under reduced pressure produced a red solid, which was heated to 70 °C for 1 h under high vacuum (ca. 10^{-3} Torr) to remove 2,2'-bipyridine by sublimation. The dark red residue was dissolved in minimal hexane and cooled to -30 °C, producing complex **1** as a red crystalline solid (0.70 g, 74% yield). Crystals suitable for single-crystal XRD were grown by slow cooling of a pentane solution. ¹H NMR (CD_2Cl_2 , 500 MHz, 293 K): $\delta = 1.61$ ppm (s, broad); attempts to observe ¹³C or ³¹P NMR signals for this complex were unsuccessful; IR (attenuated total reflectance, diamond): 2976 (m), 2932 (w), 2907 (vw, sh), 2875 (w, sh), 1474 (w), 1459 (w, sh), 1393 (m), 1369 (m), 1248 (m), 1176 (m), 1124 (m), 1103 (w), 988 (vs), 917 (w), 833 (m), 815 (w), 725 (m), 711 (m, sh), 692 (w, sh), 637 (m), 602 (m), 578 (w), 526 (s), 477 (s), 417 cm^{-1} (m); elemental analysis calcd (%) for $C_{48}H_{108}Mn_4O_{28}P_6$: C 37.5, H 7.07; found: C 37.5, H 7.03.

$[Mn_4O_4\{O_2P(pin)\}_6(bpy)_2] \cdot 0.5 CH_2Cl_2$ (2·0.5 CH_2Cl_2): The dimanganese complex $[(bpy)_2Mn(\mu_2-O)_2Mn(bpy)_2](ClO_4)_3$ (0.30 g, 0.28 mmol), $NBu_4[O_2P(pin)]$ (0.36 g, 0.84 mmol), and PPh_3 (0.074 g, 0.28 mmol) were dissolved in acetonitrile (30 mL). The dark green mixture was stirred for 24 h at room temperature. A red crystalline solid was collected by filtration and washed with acetonitrile (10 mL), diethyl ether (20 mL), toluene (40 mL), and hexane (20 mL). The product was extracted into dichloromethane solution (40 mL), which was evaporated to produce **2·0.5 CH_2Cl_2** as a red-violet solid (0.16 g, 67% yield). Crystals suitable for single-crystal XRD were grown by vapor diffusion of diethyl ether into a dichloromethane solution.

¹H NMR (CD_2Cl_2 , 500 MHz, 293 K): $\delta = 2.08$ ppm (s, broad); attempts to observe ¹³C or ³¹P NMR signals for this complex were unsuccessful; IR (attenuated total reflectance, diamond): 2981 (m), 2936 (w), 1645 (w), 1596 (m), 1577 (w), 1477 (m), 1440 (m), 1392 (m), 1372 (m), 1319 (w), 1214 (s), 1165 (w, sh), 1148 (m), 1121 (w), 1083 (vs), 1061 (s, sh), 1009 (m), 967 (s), 923 (s), 866 (s), 817 (s), 766 (s), 739 (m), 725 (s), 694 (w), 646 (s), 595 (s), 583 (w, sh), 555 (s), 526 (w, sh), 526 (s), 448 (s), 420 cm^{-1} (vw, sh); elemental analysis calcd (%) for $C_{56}H_{88}N_4Mn_4O_{26}P_6 \cdot 0.5 CH_2Cl_2$: C 40.4, H 5.33, N 3.33; found: C 40.2, H 5.19, N 3.39.

$[Mn_4O_4\{O_2P(OtBu)_2\}_6(OPEt_3)_2]$ (3): The Mn_4O_4 cubane **1** (0.26 g, 0.17 mmol) was dissolved in tetrahydrofuran (50 mL) and triethylphosphine (0.10 mL, 0.68 mmol) was added. No color change was initially observed, but the red reaction mixture gradually became more violet in color as it was stirred at room temperature over 24 h. The solvent and unreacted phosphine were removed under reduced pressure, leaving the product as a red-violet solid in apparent quantitative yield, but with silicone grease as a contaminant. The solid was dissolved in minimal hot hexane and the solution was cooled to -80 °C, affording complex **3** as a red-violet crystalline solid (0.23 g, 77% yield). Crystals suitable for single crystal XRD were grown by slow cooling of a hexane solution. ¹H NMR (CD_2Cl_2 , 500 MHz, 293 K): $\delta = 2.12$ ppm (m, broad); attempts to observe ¹³C or ³¹P NMR signals for this complex were unsuccessful; IR (attenuated total reflectance, diamond): 2974 (s), 2931 (m), 2881 (w), 1476 (m), 1458 (m), 1417 (w), 1391 (m), 1365 (s), 1296 (w), 1206 (s), 1136 (s), 1070 (vs), 1036 (s), 1010 (w, sh), 984 (vs), 916 (s), 831 (s), 779 (s), 716 (s), 684 (m), 648 (s), 614 (w, sh), 594 (m), 547 (s), 509 (m), 491 (w), 474 (s), 447 cm^{-1} (w); elemental analysis calcd (%) for $C_{60}H_{138}Mn_4O_{28}P_8$: C 40.6, H 7.84; found: C 40.9, H 7.52.

X-ray crystallographic structure determination: X-ray diffraction analysis was performed on a single crystal coated in Paratone-N oil, mounted on a Kapton loop, and transferred to a Bruker Quazar four-circle diffractometer. The crystal was cooled to 100(2) K by a stream of nitrogen gas. Data were collected using *phi* and *omega* scans with a Bruker APEX-II CCD and monochromated $Mo_{K\alpha}$ radiation ($\lambda = 0.71073$ Å). The data were integrated and corrected for Lorentz effects and polarization using Bruker APEX2 software and were corrected for absorption using SADABS (1 and 2) or TWINABS (3). Space group assignment was done by examination of systematic absences and E-statistics. The structure was solved using charge-flipping methods (SUPERFLIP, 1)^[69,70] or direct methods (SHELXS-2014, 2 and 3)^[71] and all non-hydrogen atoms were refined anisotropically using full-matrix least-squares (SHELXL-2014).^[71] Hydrogen atoms were placed in ideal positions and refined isotropically using a riding model. Because of extensive solvent disorder, SQUEEZE was used to exclude solvent electron density from the structures of **1** and **2**. Details of results for the three complexes may be found in Table 1. CCDC-1033572 (**1**), CCDC-1033571 (**2**), and CCDC-1033570 (**3**) contain the supplementary crystallographic data for this paper. These data can be obtained free of charge from The Cambridge Crystallographic Data Centre via www.ccdc.cam.ac.uk/data_request/cif

Observation of volatile thermolysis products by NMR spectroscopy: Complex **1** (0.0276 g) inside a Schlenk flask and an NMR tube containing $[D_8]$ toluene and ferrocene (0.0225 g) were connected to opposite ends of a vacuum transfer apparatus. After the system was completely evacuated, it was isolated and the NMR tube was cooled with liquid nitrogen while the flask was immersed in an oil bath at 200 ± 10 °C for 30 min. The volatile products were quantified by integrating their ¹H NMR signals against that of the ferrocene standard, after sealing the NMR tube and warming it to room temperature. To ensure accurate integrations, a long recycle delay

Table 1. Crystallographic data for compounds 1–3.

Compound	1	2	3·2C ₆ H ₁₂
empirical formula	C ₄₈ H ₁₀₈ Mn ₄ O ₂₈ P ₆	C ₅₆ H ₈₈ Mn ₄ N ₄ O ₂₆ P ₆	C ₇₂ H ₁₆₂ Mn ₄ O ₂₈ P ₈
formula weight	1538.92	1638.88	1943.53
crystal system	monoclinic	monoclinic	triclinic
space group	C2	P2 ₁ /n	P $\bar{1}$
a [Å]	35.1371(9)	14.726(3)	14.0978(8)
b [Å]	19.7817(5)	14.437(2)	14.1023(8)
c [Å]	25.0466(9)	41.650(7)	14.2236(8)
α [°]	90	90	84.144(2)
β [°]	96.7620(10)	91.877(9)	89.469(3)
γ [°]	90	90	62.213(2)
V [Å ³]	17978.3(9)	8850(2)	2486.3(2)
Z	8	4	1
ρ_{calcd} [g cm ⁻³]	1.137	1.230	1.298
μ [mm ⁻¹]	0.715	0.731	0.692
transmission max/min	0.259/0.214	0.745/0.683	0.745/0.606
crystal size [mm ³]	0.12 × 0.08 × 0.05	0.15 × 0.09 × 0.05	0.10 × 0.09 × 0.03
θ range [°]	1.167 to 25.393	1.493 to 27.268	1.441 to 25.390
rfins collected	80887	64668	8224
rfins obsd ($I_0 > 2\sigma(I_0)$)	27942	12008	6887
parameters/restraints	1690/74	889/0	578/60
R ₁ ($I_0 > 2\sigma(I_0)$)	0.0398	0.0486	0.0435
wR ₂ (all data)	0.1055	0.1206	0.1074
GOF	1.052	1.048	1.059
largest residuals [e Å ⁻³]	+0.595/−0.498	+0.825/−0.533	+0.484/−0.467

(d1) of 180 s was used following crude measurements that estimated ferrocene's relaxation time (T1) in [D₈]toluene as 41 s. For thermolysis of **1**, the products were isobutene (10.3 equivalents) and water (1.0 equivalents).

Observation of dioxygen from thermolysis by mass spectrometry: Complex **1** (0.112 g, 72.8 μmol) was placed in a round-bottomed flask connected to a 2.5 mL Teflon-stoppered sampling volume. The flask was thoroughly evacuated, charged with argon (150 Torr), and isolated. It was heated to $170 \pm 10^\circ\text{C}$ for 1 hour, then opened to the sampling volume, which had previously been evacuated. The sampling volume was then opened to an evacuated line connected to a quadrupole mass spectrometer. Calibration measurements using this vacuum system and pure sources of Ar and O₂ were used to convert the observed ion current for $m/z = 32$ (ca. 9.5×10^{-12} A), relative to the background signal ($< 2 \times 10^{-12}$ A), into an observed value in mol of O₂: 26(2) μmol , which corresponds to 0.36(2) equivalents O₂ evolved from complex **1**.

Solution-phase thermolysis of compound 1: In a typical preparation, cubane **1** (100 mg) or a mixture of cubane **1** (10 mg) and Zr[OSi(OtBu)₃]₄ or [Al(OiPr)₂O₂P(OtBu)₂]₄ (100 mg) was dissolved in anhydrous toluene (3 mL). In a sealed vessel, the mixture was heated to 160 °C for 20–30 min, during which time the dark red solution changed to a light brown gel. Removal of solvent under reduced pressure produced a light brown solid. Calcination was performed in a temperature-controlled tube furnace under flowing O₂.

X-ray absorption spectroscopy: X-ray absorption spectra were taken at the Advanced Light Source (ALS) on Beamline 10.3.2. The radiation was monochromatized by a Si(111) double-crystal monochromator. The intensity of the incident X-ray (I_0) was monitored by an N₂-filled ionization chamber in front of the sample. The energy was calibrated using a glitch in I_0 relative to the absorption edge of an Mn foil. All data were collected at room temperature using a quick XAS scan mode, and the data collection was carried out under the threshold of X-ray radiation damage, by monitoring with the XANES edge shift. Data reduction was performed using

custom software (Matthew Markus, BL 10.3.2, ALS). Pre-edge and post-edge contributions were subtracted from the XAS spectra and the result was normalized with respect to the edge jump. Details of EXAFS fitting may be found in the Supporting Information.

Acknowledgements

J. M. Zadrozny and J. R. Long (magnetic susceptibility), A. T. Iavarone (ESI-TOF-MS), M. S. Ziegler (single-crystal XRD), and W. Kim and H. Frei (MS detection of O₂) are gratefully acknowledged for their contributions in characterizing the compounds herein. This material is based upon work performed by the Joint Center for Artificial Photosynthesis, a DOE Energy Innovation Hub, supported through the Office of Science of the U.S. Department of Energy under Award Number DE-SC0004993. K.M.V. acknowledges support from a National Science Foundation Graduate Research Fellowship under Grant No. DGE-1106400. Single-crystal X-ray structure determination was supported by NIH Shared Instrumentation Grant S10-RR027172. The Advanced Light Source is supported by the Director, Office of Science, Office of Basic Energy Sciences, of the U.S. Department of Energy under Contract No. DE-AC02-05CH11231.

Keywords: artificial photosynthesis · cubanes · oxygen-atom transfer · thermolytic molecular precursor · water oxidation

- [1] Y. Umena, K. Kawakami, J.-R. Shen, N. Kamiya, *Nature* **2011**, *473*, 55–60.
- [2] M. W. Kanan, J. Yano, Y. Surendranath, M. Dincă, V. K. Yachandra, D. G. Nocera, *J. Am. Chem. Soc.* **2010**, *132*, 13692–13701.
- [3] M. Risch, V. Khare, I. Zaharieva, L. Gerencser, P. Chernev, H. Dau, *J. Am. Chem. Soc.* **2009**, *131*, 6936–6937.
- [4] S. W. Gersten, G. J. Samuels, T. J. Meyer, *J. Am. Chem. Soc.* **1982**, *104*, 4029–4030.
- [5] J. McEvoy, G. W. Brudvig, *Chem. Rev.* **2006**, *106*, 4455–4483.
- [6] J. Barber, J. W. Murray, *Philos. Trans. R. Soc. B* **2008**, *363*, 1129–1138.
- [7] G. W. Brudvig, *Philos. Trans. R. Soc. B* **2008**, *363*, 1211–1219.
- [8] K. Meelich, C. M. Zaleski, V. L. Pecoraro, *Philos. Trans. R. Soc. B* **2008**, *363*, 1271–1281.
- [9] P. Siegbahn, *Acc. Chem. Res.* **2009**, *42*, 1871–1880.
- [10] R. H. Holm, *Chem. Rev.* **1987**, *87*, 1401–1449.
- [11] F. Liu, J. J. Concepcion, J. W. Jurss, T. Cardolaccia, J. L. Templeton, T. J. Meyer, *Inorg. Chem.* **2008**, *47*, 1727–1752.
- [12] J. K. Hurst, J. L. Cape, A. E. Clark, S. Das, C. Qin, *Inorg. Chem.* **2008**, *47*, 1753–1764.
- [13] B. S. Lane, K. Burgess, *Chem. Rev.* **2003**, *103*, 2457–2474.
- [14] G. B. Shul'pin, *J. Mol. Catal. A* **2002**, *189*, 39–66.
- [15] E. Roduner, W. Kaim, B. Sarkar, V. B. Urlacher, J. Pleiss, R. Gläser, W. D. E. E. Roduner, G. A. Sprenger, U. Beifuß, E. Klemm, C. Liebner, H. Hieronymus, S.-F. Hsu, B. Plietker, S. Laschat, *ChemCatChem* **2013**, *5*, 82–112.
- [16] P. Tang, Q. Zhu, Z. Wu, D. Ma, *Energy Environ. Sci.* **2014**, *7*, 2580–2591.
- [17] R. S. Drago, *Coord. Chem. Rev.* **1992**, *117*, 185–213.
- [18] W. Ruettinger, C. Campana, G. Dismukes, *J. Am. Chem. Soc.* **1997**, *119*, 6670–6671.
- [19] T. Carrell, S. Cohen, G. Dismukes, *J. Mol. Catal. A* **2002**, *187*, 3–15.
- [20] W. Ruettinger, M. Yagi, K. Wolf, S. Bernasek, G. Dismukes, *J. Am. Chem. Soc.* **2000**, *122*, 10353–10357.
- [21] W. Ruettinger, G. Dismukes, *Inorg. Chem.* **2000**, *39*, 1021–1027.
- [22] M. Yagi, K. Narita, *J. Am. Chem. Soc.* **2004**, *126*, 8084–8085.

- [23] K. Narita, T. Kuwabara, K. Sone, K.-I. Shimizu, M. Yagi, *J. Phys. Chem. B* **2006**, *110*, 23107–23114.
- [24] E. M. W. Rumberger, H. S. Ahn, A. T. Bell, T. D. Tilley, *Dalton Trans.* **2013**, *42*, 12238–12247.
- [25] G. P. Gardner, Y. B. Go, D. M. Robinson, P. F. Smith, J. Hadermann, A. Abakumov, M. Greenblatt, G. C. Dismukes, *Angew. Chem. Int. Ed.* **2012**, *51*, 1616–1619; *Angew. Chem.* **2012**, *124*, 1648–1651.
- [26] P. F. Smith, C. Kaplan, J. E. Sheats, D. M. Robinson, N. S. McCool, N. Mezle, G. C. Dismukes, *Inorg. Chem.* **2014**, *53*, 2113–2121.
- [27] C. G. Lugmair, T. D. Tilley, A. L. Rheingold, *Chem. Mater.* **1997**, *9*, 339–348.
- [28] K. W. Terry, C. G. Lugmair, T. D. Tilley, *J. Am. Chem. Soc.* **1997**, *119*, 9745–9756.
- [29] C. G. Lugmair, T. D. Tilley, *Inorg. Chem.* **1998**, *37*, 6304–6307.
- [30] C. G. Lugmair, T. D. Tilley, A. L. Rheingold, *Chem. Mater.* **1999**, *11*, 1615–1620.
- [31] J. W. Kriesel, M. S. Sander, T. D. Tilley, *Adv. Mater.* **2001**, *13*, 331–335.
- [32] J. W. Kriesel, M. S. Sander, T. D. Tilley, *Chem. Mater.* **2001**, *13*, 3554–3563.
- [33] K. L. Fajdala, T. D. Tilley, *J. Catal.* **2003**, *218*, 123–134.
- [34] K. L. Fajdala, A. G. Oliver, F. J. Hollander, T. D. Tilley, *Inorg. Chem.* **2003**, *42*, 1140–1150.
- [35] K. L. Fajdala, T. D. Tilley, *Chem. Mater.* **2004**, *16*, 1035–1047.
- [36] K. L. Fajdala, R. L. Brutchey, T. D. Tilley in *Topics in Organometallic Chemistry* (Eds.: C. Copéret, B. Chaudret), Springer, Berlin, Heidelberg, **2005**, pp. 69–115.
- [37] H. S. Ahn, T. D. Tilley, *Adv. Funct. Mater.* **2013**, *23*, 227–233.
- [38] R. Murugavel, M. Sathiyendiran, M. G. Walawalkar, *Inorg. Chem.* **2001**, *40*, 427–434.
- [39] M. Sathiyendiran, R. Murugavel, *Inorg. Chem.* **2002**, *41*, 6404–6411.
- [40] R. Pothiraja, M. Sathiyendiran, R. J. Butcher, R. Murugavel, *Inorg. Chem.* **2004**, *43*, 7585–7587.
- [41] R. Murugavel, A. Choudhury, M. G. Walawalkar, R. Pothiraja, C. N. R. Rao, *Chem. Rev.* **2008**, *108*, 3549–3655.
- [42] R. Murugavel, S. Kuppuswamy, N. Gogoi, R. Boomishankar, A. Steiner, *Chem. Eur. J.* **2010**, *16*, 994–1009.
- [43] F. Meyer, R. Hempelmann, S. Mathur, M. Veith, *J. Mater. Chem.* **1999**, *9*, 1755–1763.
- [44] K. C. Kumara Swamy, M. Veith, V. Huch, S. Mathur, *Inorg. Chem.* **2003**, *42*, 5837–5843.
- [45] M. P. Coles, C. G. Lugmair, K. W. Terry, T. D. Tilley, *Chem. Mater.* **2000**, *12*, 122–131.
- [46] R. L. Brutchey, B. V. Mork, D. J. Sirbuly, P. Yang, T. D. Tilley, *J. Mol. Catal. A* **2005**, *238*, 1–12.
- [47] R. L. Brutchey, D. A. Ruddy, L. K. Andersen, T. D. Tilley, *Langmuir* **2005**, *21*, 9576–9583.
- [48] D. A. Ruddy, T. D. Tilley, *Chem. Commun.* **2007**, 3350–3352.
- [49] L. Raboin, J. Yano, T. D. Tilley, *J. Catal.* **2012**, *285*, 168–176.
- [50] S. Cooper, M. Calvin, *J. Am. Chem. Soc.* **1977**, *99*, 6623–6630.
- [51] A. Zwierzak, M. Kluba, *Tetrahedron* **1971**, *27*, 3163–3170.
- [52] N. E. Chakov, K. A. Abboud, L. N. Zakharov, A. L. Rheingold, D. N. Hendrickson, G. Christou, *Polyhedron* **2003**, *22*, 1759–1763.
- [53] J.-Z. Wu, E. Sellitto, G. P. A. Yap, J. Sheats, G. C. Dismukes, *Inorg. Chem.* **2004**, *43*, 5795–5797.
- [54] J. Vincent, C. Christmas, H. Chang, Q. Li, P. Boyd, J. Huffman, D. Hendrickson, G. Christou, *J. Am. Chem. Soc.* **1989**, *111*, 2086–2097.
- [55] J. S. Kanady, J. L. Mendoza-Cortes, E. Y. Tsui, R. J. Nielsen, W. A. Goddard III, T. Agapie, *J. Am. Chem. Soc.* **2013**, *135*, 1073–1082.
- [56] A. W. Addison, T. N. Rao, J. Reedijk, J. van Rijn, G. C. Verschoor, *J. Chem. Soc. Dalton Trans.* **1984**, 1349–1356.
- [57] R. J. Kulawiec, R. H. Crabtree, G. W. Brudvig, *Inorg. Chem.* **1988**, *27*, 1309–1311.
- [58] J. B. Vincent, G. Christou, *Inorg. Chim. Acta* **1987**, *136*, L41–L43.
- [59] G. Christou, J. B. Vincent, *Biochim. Biophys. Acta* **1987**, *895*, 259–274.
- [60] V. K. Yachandra, K. Sauer, M. P. Klein, *Chem. Rev.* **1996**, *96*, 2927–2950.
- [61] S. Mukhopadhyay, S. K. Mandal, S. Bhaduri, W. H. Armstrong, *Chem. Rev.* **2004**, *104*, 3981–4026.
- [62] H. Dau, C. Limberg, T. Reier, M. Risch, S. Roggan, P. Strasser, *ChemCatChem* **2010**, *2*, 724–761.
- [63] R. Glaum, H. Thauern, A. Schmidt, M. Gerk, *Z. Anorg. Allg. Chem.* **2002**, *628*, 2800–2808.
- [64] T. Stefanidis, A. G. Nord, *Acta Crystallogr. Sect. C* **1984**, *40*, 1995–1999.
- [65] K. W. Terry, T. D. Tilley, *Chem. Mater.* **1991**, *3*, 1001–1003.
- [66] J. S. Kanady, R. Tran, J. A. Stull, L. Lu, T. A. Stich, M. W. Day, J. Yano, R. D. Britt, T. Agapie, *Chem. Sci.* **2013**, *4*, 3986–3996.
- [67] V. Manev, N. Ilchev, A. Nassalevska, *J. Power Sources* **1989**, *25*, 167–175.
- [68] T. Modro, J. Sokolowski, *Zesz. Nauk. Wyzsz. Szk. Pedagog. Gdansk. Mat. Fiz.* **1965**, *5*, 77–80.
- [69] G. Oszlányi, A. Sütő, *Acta Crystallogr. Sect. A* **2004**, *60*, 134–141.
- [70] L. Palatinus, G. Chapuis, *J. Appl. Crystallogr.* **2007**, *40*, 786–790.
- [71] G. M. Sheldrick, *Acta Crystallogr. Sect. A* **2008**, *64*, 112–122.

Received: November 16, 2014

Published online on February 11, 2015